Anal. Chem. **1999,** *71,* 1521−1528

Determination of Low-*Z* Elements in Individual Environmental Particles Using Windowless EPMA

Chul-Un Ro,[†] János Osán,[‡,§] and René Van Grieken*[,‡]

Department of Chemistry, University of Antwerp (UIA), Universiteitsplein 1, B-2610 Antwerpen, Belgium, and Department of Chemistry, Hallym University, ChunCheon, KangWonDo, 200-702, Korea

The determination of low-*Z* elements such as carbon, nitrogen, and oxygen in atmospheric aerosol particles is of interest in studying environmental pollution. Conventional electron probe microanalysis technique has a limitation for the determination of the low-*Z* elements, mainly because the Be window in an energy-dispersive X-ray (EDX) detector hinders the detection of characteristic X-rays from light elements. The feasibility of low-*Z* element determination in individual particles using a windowless EDX detector is investigated. To develop a method capable of identifying chemical species of individual particles, both the matrix and the geometric effects of particles have to be evaluated. X-rays of low-*Z* elements generated by an electron beam are so soft that important matrix effects, mostly due to X-ray absorption, exist even within particles in the micrometer size range. Also, the observed radiation, especially that of light elements, experiences different extents of absorption, depending on the shape and size of the particles. Monte Carlo calculation is applied to explain the variation of observed X-ray intensities according to the geometric and chemical compositional variation of individual particles, at different primary electron beam energies. A comparison is carried out between simulated and experimental data, collected for standard individual particles with chemical compositions as generally observed in marine and continental aerosols. Despite the many fundamental problematic analytical factors involved in the observation of X-rays from low-*Z* elements, the Monte Carlo calculation proves to be quite reliable to evaluate those matrix and geometric effects. Practical aspects of the Monte Carlo calculation for the determination of light elements in individual particles are also considered.

Studying atmospheric pollution is of high importance, not only in continental but also in maritime regions. For example, it has been found that up to 50% of some of the heavy metal pollution of the North Sea comes from the deposition of the coarse atmospheric aerosol particles.[1,2] It has recently also been recognized that, for example, an important fraction of the enhanced supply of nutrients (both major nutrients and essential elements), which is causing eutrophication problems in the Southern Bight of the North Sea, may be related to air pollution (e.g., nitrogen oxides from traffic pollution and ammonia from agricultural emissions being transformed to and deposited as nitrates and ammonium compounds).[3] The biological impact and the health hazards of heavy metals and nutrients are often studied by transport models, which calculate the atmospheric concentration and deposition, but these need accurate input data. The atmospheric behavior of airborne and depositing particles is determined not only by their composition but also by their morphology. Since the atmospheric particles are chemically and morphologically heterogeneous, and the average composition and the average aerodynamic diameter do not describe well the population of the particles, advanced analytical chemistry methods are necessary, such as microanalytical methods. Concerning the biological impact of the deposited particles, the surface layers of the particles will be more in contact with water after the deposition step and, thus, more amenable to dissolution and biological action, and surface sensitive techniques are important in this sense too. Electron probe X-ray microanalysis (EPMA) is capable of simultaneously detecting the chemical composition and morphology of a microscopic volume as a single atmospheric particle.[4−7]

Both for chemical speciation at the single-particle level and for adequate identification of nutrients, major elements such as carbon, nitrogen, and oxygen must be detected; they form the major mass of aerosols, and major nutrients are generally nitrogen-rich. This is not possible by EPMA with conventional detectors. However, using an electron microprobe, which can be operated in windowless mode, very low energy X-rays can be detected and give at least qualitative information about the low-*Z* components. In this work, the feasibility of semiquantitative light element analysis using windowless EPMA is investigated.

In the literature, only three preliminary articles have appeared hitherto on the use of windowless EPMA for the analysis of

* Corresponding author: (fax) +32 3 820 2376; (e-mail) vgrieken@uia.ua.ac.be.
[†] Hallym University.
[‡] University of Antwerp (UIA).
[§] On leave from: KFKI Atomic Energy Research Institute, P.O. Box 49, H-1525 Budapest, Hungary.

(1) Van Malderen, H.; Rojas, C.; Van Grieken, R. *Environ. Sci. Technol.* **1992**, *26*, 750−756.
(2) Injuk, J.; Van Grieken, R. *J. Atmos. Chem.* **1995**, *20*, 179−212.
(3) Prospero, J. M.; Barrett, K.; Church, T.; Dentener, F.; Duce, R. A.; Galloway, J. N.; Levy, H., II; Moody, J.; Quinn, P. *Biogeochemistry* **1996**, *35*, 27−73.
(4) Török, Sz.; Sándor, Sz.; Xhoffer, C.; Van Grieken, R.; Mészáros, E.; Molnár, Á. *Idôjárás* **1992**, *96*, 223−233.
(5) Osán, J.; Török, Sz.; Török, K.; Németh, L.; Lábár, J. L. *X-Ray Spectrom.* **1996**, *25*, 167−172.
(6) Van Grieken, R.; De Bock, L.; Hoornaert, S.; Jambers, W.; Koutsenogii P. In *Preservation of Our World in the Wake of Change*; Steinberger, Y., Ed.; ISEEQS Publication: Jerusalem, 1996; Vol. 6A, pp 67−70.
(7) Jambers, W.; Van Grieken, R. *Environ. Sci. Technol.* **1997**, *31*, 1525−1533.

10.1021/ac981070f CCC: $18.00
Published on Web 03/06/1999

environmental individual particles, but not even semiquantitative compositions were derived for light elements. This is because of the fundamental analytical problems that still must be solved before the technique can be applied in environmental research; X-rays generated by the electron beam in low-*Z* elements are so soft that important matrix effects (mostly due to X-ray absorption) exist even within particles in the micrometer size range and also those photons experience different matrix effects among particles with different size and shape (geometric effect).

Almost a decade ago, Bishop et al.[8] used the scanning electron microscope (SEM) equipped with ultrathin window energy-dispersive X-ray (EDX) detector for light element X-ray microanalysis of sedimentary organic particles. From their measurements on polished and carbon-coated samples, the authors claimed that this light element analysis allowed qualitative assessment of the carbon, oxygen, sulfur, and chlorine contents of individual sedimentary organic particles.

The first results of the application of windowless SEM/EDX for light element analysis of single aerosol particles was published by Hamilton et al.[9] The authors were interested in the detection of airborne carbonaceous material, so they chose an appropriate filter material for carbon determination, namely, the Whatman Anodisc alumina-based membrane filter. Since the chosen ceramic filter material is nonconductive, gold sputtering was used to give conductive coating to the samples. Due to the oxygen background of the substrate and the additional absorption introduced by the gold coating, their method was only suitable for qualitative carbon determination. The classification of airborne particles was based only on net intensities of characteristic X-ray lines, without considering matrix and geometric effects.

Fruhstorfer and Niessner[10] analyzed airborne particles collected on conventional Nuclepore membrane filters. The samples received a 15-nm silver coating, because the silver X-ray lines do not overlap with those of the elements of interest. For the classification of airborne particles, different standard particles with compositions commonly observed in the aerosol were prepared and measured at the same instrumental conditions as the aerosol samples. The authors claimed that the method proved the identification of soot particles having a diameter as low as 50 nm, and their spectra could be distinguished from those of other particles or pure substrate in 500-ms live-time measurements. However, they used a relatively high current (1−2 μA) at 25 kV, possibly causing damage to submicrometer particles even within milliseconds. The classification of the particles was done by comparing the spectra of the unknown particles with those of the standards, and thus no quantitative analysis was attempted.

Another possibility is the application of wavelength-dispersive X-ray (WDX) detection for semiquantitative light element analysis of individual aerosol particles. It was shown recently by Weinbruch et al.[11] that semiquantitative WDX analysis, down to oxygen, is feasible even for irregularly shaped particles down to 0.8 μm in equivalent diameter. The elemental concentrations were calculated using the particle ZAF correction of Armstrong,[12] providing good results for silicate particles. Although the peak-to-background ratio of WDX is essentially better than that of EDX by use of layered crystals with high reflectivity, and the overlapping between light element K-lines and L-lines of transition metals present in the particle is much less pronounced due to the superior energy resolution of WDX, the high current needed for the measurements limits its possibilities to the most stable particles under electron bombardment (e.g., silicate particles).

The ultimate goal of our research is the speciation of both major nutrients and toxic heavy metals in individual aerosol particles using computer-controlled EPMA; it is impossible to achieve the objective without at least semiquantitative analysis of major, low-*Z* elements. The present research aims to develop a microanalytical method based on EPMA using a windowless EDX detector, which allows light element detection in individual microparticles. The development of a method to compensate for the matrix and geometric effects, which are even the most pronounced for light element X-rays, is of primary interest in this work.

Most of the correction methods used in quantitative EPMA, such as ZAF and $\phi(\rho z)$-based methods requires perfectly flat sample surface and homogeneous composition to avoid geometric effects. In the case of single-particle analysis, however, it is essential to compensate for the geometric effect. In the past two decades, several research groups dealt with the theoretical evaluation of the matrix and geometric effects in individual particles.[13,14] The employed correction methods are based on the calculation of *k*-ratios, obtained from the unknown composition particles and bulk standards. The accuracy of the correction procedures depends largely on the quality of the assumed X-ray generation depth function [$\phi(\rho z)$]. Several different methods of quantitative analysis of microparticles were critically reviewed by Armstrong.[12] The particle ZAF methods based on bulk standards introduce large errors for the light elements, mostly because of the large absorption correction needed for the low-*Z* elements and the difference between the behavior of bulk samples and single particles under electron bombardment. Also, when the average atomic number of the substrate differs significantly from that of the particle, the side-scattering correction of the $\phi(\rho z)$ function is reasonable only if the electron excitation volume is smaller than the particle itself. Therefore, in general, this method cannot be used to accurately analyze submicrometer particles.[12] Monte Carlo calculation combined with measurements on particulate standards may be only a promising method if light element analysis is needed or the particles are sensitive to the electron beam.

EXPERIMENTAL SECTION

Samples. For the evaluation of the matrix and geometric effects, particulate standards were prepared and measured. The standard particles were prepared by grinding pro analysis grade solid chemical compounds to microscopic size using an agate mortar. Chemical compounds, generally present in atmospheric aerosol particles, were selected: $CaCO_3$, $CaSO_4 \cdot 2H_2O$, $BaSO_4$, SiO_2, Fe_2O_3, and NaCl.

(8) Bishop, A. N.; Kearsley, A. T.; Patience, R. L. *Org. Geochem.* **1992**, *18*, 431−446.

(9) Hamilton, R. S.; Kershaw, P. R.; Segarra, F.; Spears C. J.; Watt, J. M. *Sci. Total Environ.* **1994**, *146/147*, 303−308.

(10) Fruhstorfer, P.; Niessner, R. *Mikrochim. Acta* **1994**, *113*, 239−250.

(11) Weinbruch, S.; Wentzel, M.; Kluckner, M.; Hoffman, P.; Ortner, H. M. *Mikrochim. Acta* **1997**, *125*, 137−141.

(12) Armstrong, J. T. In *Electron Probe Quantitation*; Heinrich K. F. J., Newbury, D. E., Eds.; Plenum Press: New York, 1991; pp 261−316.

(13) Armstrong, J. T.; Buseck, P. R. *X-Ray Spectrom.* **1985**, *14*, 172−182.

(14) Storms, H. M.; Janssens, K. H.; Török, S. B.; Van Grieken, R. E. *X-Ray Spectrom.* **1989**, *18*, 45−52.

To avoid the additional absorption and the spectral overlap possibly caused by the conductive coating of the sample, metallic substrates such as aluminum and indium foils were used for the collection of the standard particles, without further conductive coating. The particles were suspended in 0.01 M methanol, pipetted onto the metallic foils, and dried in the air before EPMA analysis.

EPMA Measurements. The measurements were carried out on a JEOL 6300 SEM equipped with a PGT EDX detector. The Si(Li) detector can be operated in windowless mode and its resolution is 170 eV for Mn Kα X-rays. The vacuum system of the SEM consists of oil rotary (one unit) and oil diffusion pumps (two units). To reduce the deposition of the oil residues to the sample and the detector, a continuous cleaned N_2 gas flow was applied. Since the generation volume of X-rays depends on the energy of the primary electron beam and low-energy X-ray photons experience different absorption, depending on the positions of their generation, the measurements were done at 5-, 10-, and 20-kV accelerating voltages for all of the standard samples, to find the optimal experimental conditions for light element analysis. The typical beam current was 1 nA for all the accelerating voltages. The shape and the size of individual microparticles were obtained from their secondary electron images collected at 0 and 60° tilts of the sample stage. These estimated geometrical data were used in the Monte Carlo simulations.

Monte Carlo Simulations. To simulate the electron trajectories in microparticles sitting on a flat substrate and the production and absorption of X-rays, a modified CASINO Monte Carlo program was used. The ANSI standard C code CASINO program, developed by Hovington et al.,[15] is a single-scattering Monte Carlo calculation, especially designed for low-energy beam interactions in bulk, thin foil, and the spherical inclusions with homogeneous composition.[16] The CASINO program can be used either on a DOS-based PC or on a UNIX-based workstation. This program employs tabulated Mott elastic cross sections and experimentally determined stopping powers. Function pointers are used for the most essential routines so that different physical models can easily be implemented. The program can simulate several types of signals, such as X-rays and secondary and backscattered electrons, as a point analysis, as a line scan, or as an image format, for accelerating voltages between 0.1 and 30 kV.

The CASINO program was modified to meet the needs of the present study. The original program can deal with a spherical inclusion embedded in a substrate, but the surface of the whole sample must be flat. The modification of the program by us allows the simulation of electron trajectories in spherical, hemispherical, and hexahedral particles sitting on a flat surface (Figure 1). The simulation of X-ray spectra and Bremsstrahlung background are also implemented. The parametrization of Kirkpatrick and Weidmann[17] is used for the background calculation. However, the simulation including the calculation of Bremsstrahlung takes more CPU time than without it.

RESULTS AND DISCUSSION

Collecting Substrate. Thin-film coating of carbon or metals on insulating samples is commonly used to reduce charging during EPMA measurements. Since the absorption of low-energy X-rays is much more pronounced, conductive coating of the sample is not desirable. Conductive carbon coating could introduce large inaccuracy in the determination of carbon in the particle. L X-ray lines of metallic coatings often overlap with characteristic lines of light elements so that the X-ray intensities of low-*Z* elements can only be estimated inaccurately. Also, the presence of the metallic coating reduces the X-ray intensities, especially of low-energy photons, due to their absorption in the coating material. Nuclepore filters, which are polycarbonate filters and ideal for computer-controlled EPMA because of their microscopically flat surface, cannot be used as a collecting substrate for the analysis of carbon and oxygen, because the filters are composed of carbon and oxygen. Furthermore, the use of these filters as a collecting substrate requires conductive coating. In this study, aluminum and indium foils were examined to investigate their suitability as collecting substrates, without conductive coating. It was found that indium foil is not a suitable collecting substrate for low-*Z* element analysis; the metal is so soft that many particles are often embedded in it, making the analysis difficult, and also indium metal produces strong Bremsstrahlung signals which overlap with the characteristic lines of nitrogen and oxygen (Figure 2). Even though aluminum metal substrates obviously hinder the determination of the aluminum element in particles, aluminum foil was used as a collecting substrate in this work.

Choice of Primary Electron Beam Energy. The X-ray spectra of each particle were measured at three different energies of primary electron beam, 5, 10, and 20 kV, to determine which electron beam energy provides the best analytical signal, especially for light element analyses. In general, the generation volume of light element X-rays is more similar to the excitation volume of the electron beam because their ionization energies are less than those of elements detected by the conventional EPMA technique. For example, the calculated Kenaya−Okayama electron excitation range for $CaCO_3$ is 0.4 μm at 5-kV electron accelerating voltage. Using Anderson−Hasler equations, the X-ray generation ranges at 5-kV electron accelerating voltage are calculated as 0.3 μm for carbon and oxygen and 0.1 μm for calcium in $CaCO_3$.[18] Carbon and oxygen Kα photons are generated in a volume similar to that of the excitation, whereas other characteristic lines, such as those of calcium and sulfur, are generated in a shallower region. Also, of course, more X-rays are generated in deep regions inside the sample as the energy of the electron beam increases. Therefore, with increasing energy of the electron beam, low-energy X-rays are generated at deeper regions than higher energy X-rays. Because low-energy photons are strongly absorbed while they travel through the sample (e.g., example, the attenuation length of oxygen Kα photons is just 0.3 μm in $CaCO_3$), the characteristic radiation of light elements coming from the shallow region is detectable. In this context, the 5-kV electron beam, among the three beam energies, provides the strongest intensities of low-energy X-rays. In contrast, the higher energy X-rays are produced most strongly at 20-kV electron accelerating voltage.

The generation volume of X-rays and the excitation volume of electrons can be larger than that of microparticles, depending on

(15) Hovington, P.; Drouin, D.; Gauvin, R. *Scanning* **1997**, *19*, 1−14.
(16) Gauvin, R.; Hovington, P.; Drouin, D. *Scanning* **1995**, *17*, 202−219.
(17) Kirkpatrick, P.; Weidmann, L. *Phys. Rev.* **1945**, *67*, 321−339.
(18) Goldstein, J. I.; Newbury, D. E.; Echlin, P.; Joy, D. C.; Romig, A. D., Jr.; Lyman, C. E.; Fiori, C.; Lifshin, E. *Scanning Electron Microscopy and X-Ray Microanalysis*; 2nd ed.; Plenum Press: New York, 1992.

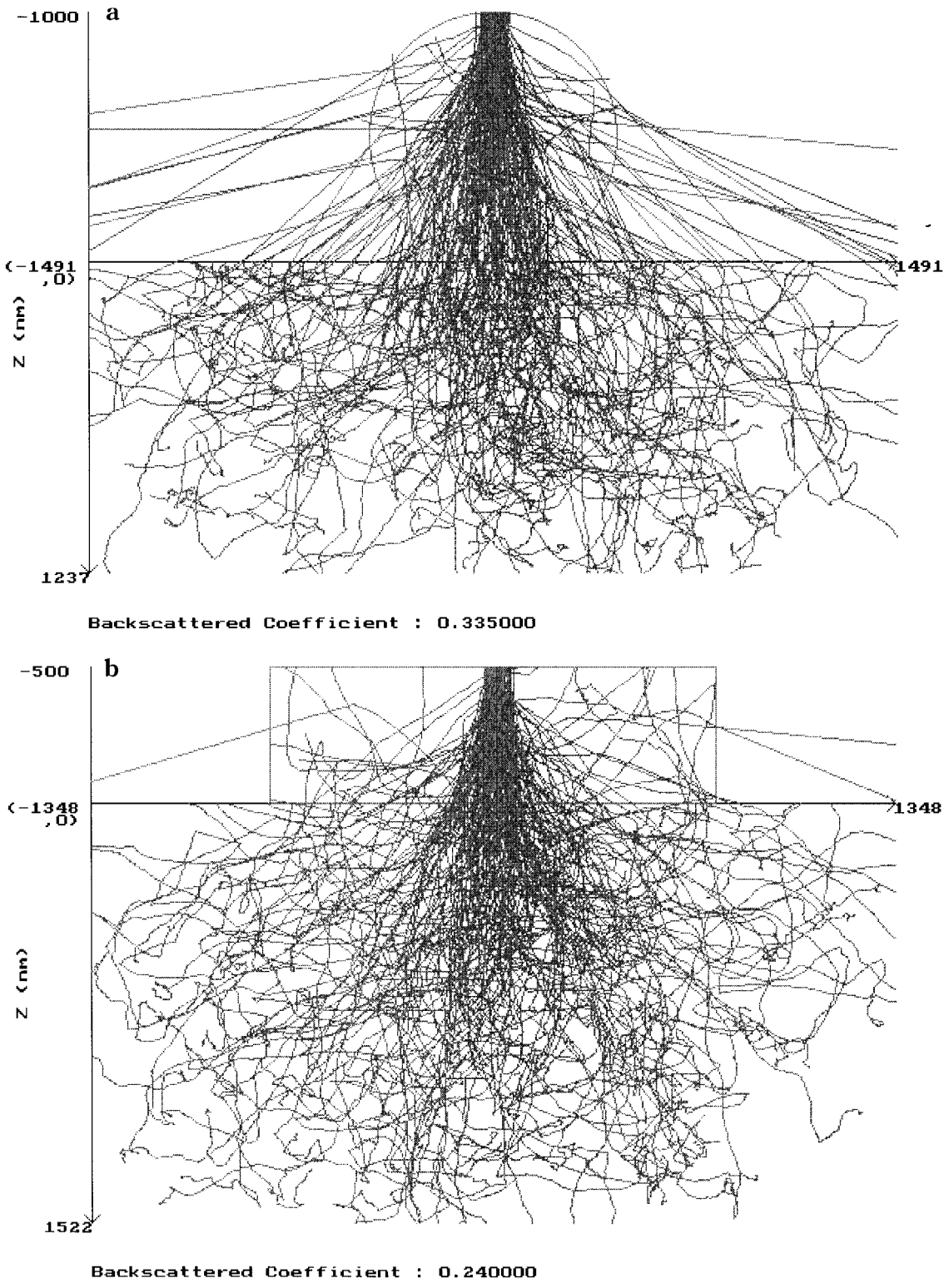

Figure 1. Simulation of electron trajectories in (a) spherical and (b) hexahedral particles.

the beam energy and the size of particles, so that the detected X-ray intensities can be different from those for a bulk specimen with a flat surface. The influence of the particle size effect on X-ray spectra and elemental characteristic intensities of microparticles was studied by performing intensive simulations for particles of size ranging from 0.1 to 10 μm. Simulations were done for 5-, 10-, and 20-kV accelerating voltages and all of the studied compounds. As an example, the simulated intensities as a function of particle diameter, at the different electron beam energies and for spherical $CaCO_3$ particles, are presented in Figure 3. The decrease of the characteristic intensities of carbon, oxygen, and calcium is more pronounced in the submicrometer size range, at the three different electron beam energies, where the excitation volume is larger than the volume of the particle. For sizes of a few tenths of a micrometer, the decrease is the most drastic, because the size of the particle and the beam diameter starts to become comparable.

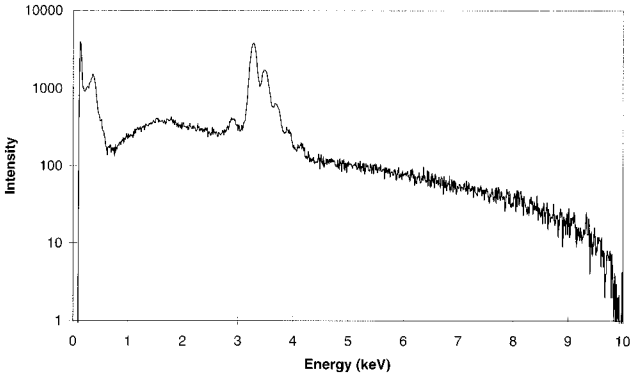

Figure 2. X-ray spectrum of indium foil at 10-kV accelerating voltage.

At 5- and 10-kV accelerating voltages, the X-ray intensities of carbon, oxygen, and calcium for the particles larger than 1 μm size are almost the same in their magnitudes; the excitation volumes are smaller than those of the particles at the 5- and 10-kV beam energies (Figure 3a and b, respectively). At 20 kV, the excitation volumes are comparable with or larger than the sample volumes at this size range, and thus the X-ray intensities of carbon, oxygen, and calcium increase as the particle size increases.

For particles of a size larger than 1 μm, the intensities of carbon and oxygen are comparable at 5 and 10 kV, whereas the intensities at 20 kV are smaller than those at 5 and 10 kV (Figure 3). As the electron beam energy increases, light element X-rays are generated deeper in the particles, absorbed more while they travel through the particles, and detected less. For particles of very small size (0.1−0.2-μm diameter), the intensities of carbon and oxygen are comparable at 10 and 20 kV and smaller at 5 kV. Since the excitation volume is larger than the particle itself, most of the electrons are traveling into the aluminum substrate. A part of them is backscattered to the particle, and yet the backscattered electrons already lost some of their energy. The X-ray intensities of light elements at 5 kV may be lower because the number of backscattered electrons, which can excite carbon and oxygen, are less at 5 kV.

The X-ray signal of the aluminum substrate is predominant at the 20-kV electron beam. For smaller particles, the aluminum intensity is the strongest because most of the primary electrons penetrate into the substrate. As the energy of the electron beam decreases, the aluminum X-rays become less dominating.

Among the three accelerating voltages, the 10-kV electron beam is optimal for light element analysis. It provides a considerable amount of X-rays of the light elements, with minimal dependence on the size variation of microparticles. The magnitude of the intensities is comparable with that at 5 kV for light elements and also with that at 20 kV for the other elements. The X-ray intensity of the aluminum substrate is also compromised at the 10-kV electron beam.

Determination of the Geometry of Particles. Since the accurate geometry of the particles is crucial in the Monte Carlo calculation, secondary electron images were recorded to determine the size and shape of the particles. If a particle is perfectly spherical, it is possible to determine its diameter accurately from one secondary electron image, even though the secondary image of the particle is a projection of a three-dimensional sphere onto a two-dimensional plane. However, when the geometry of hexahedral particles is to be determined, at least two secondary electron images, taken at different sample tilts, are required to determine their three-dimensional geometry. In this work, two secondary electron images of each particle were acquired at 0 and 60° sample stage tilts. If a hexahedral particle sits on a flat substrate and thus only the top surface of the particle is seen in the image taken at the 0° tilt, the real size of the top surface is the same as the one in the image and the height of the particle is determined by measuring its height from the image at the 60° tilt;

$$H = H_{60}/\sin 60° \qquad (1)$$

where H is the real height and H_{60} is the height measured from the image taken at 60° tilt.

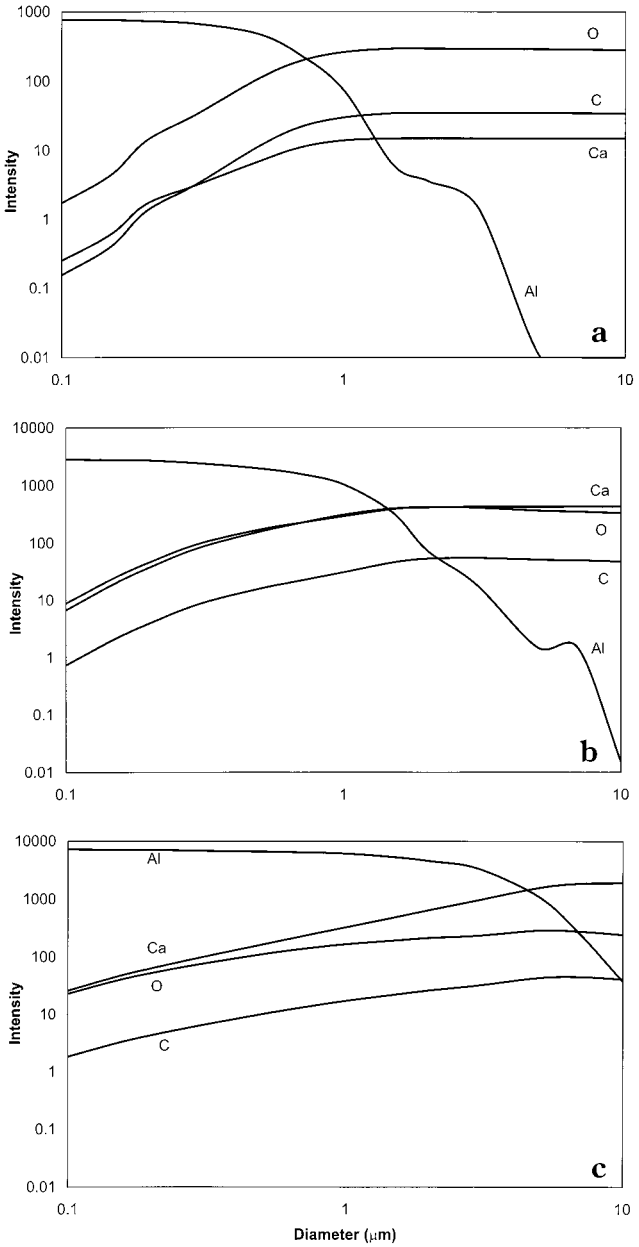

Figure 3. Spherical $CaCO_3$ particles: variation of X-ray intensities according to particle diameter at (a) 5-, (b) 10-, and (c) 20-kV accelerating voltage.

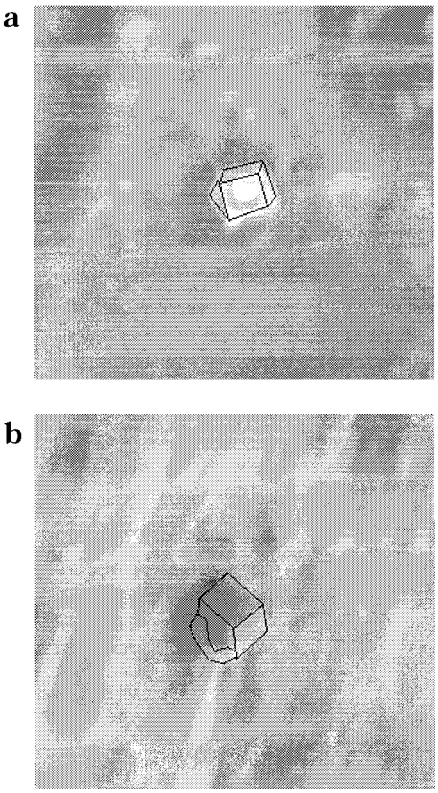

Figure 4. Secondary electron images of a $CaCO_3$ particle at (a) 0 and (b) 60° sample tilt. (For clarity, solid lines are added in images along the sides.)

When a hexahedral particle does not sit on the flat surface, which occurs frequently for microscopically nonflat aluminum foils, all three sides of the particle are seen in the images at both 0 and 60° tilts, as shown in Figure 4. In this case, the real size of each side is determined using eq 2, where R is the real size, R_0

$$R^2 = R_0^2 + \frac{3}{4}(R_{60}^2 - R_0^2 \sin^2\theta) + \frac{1}{3}R_0^2 \cos^2\theta - \frac{4}{3}R_0 \cos\theta (R_{60}^2 - R_0^2 \sin^2\theta)^{1/2} \quad (2)$$

and R_{60} are the sizes at the images of the 0 and 60° tilts, respectively, and θ is the angle, at the image of the 0° tilt, between the perpendicular axis to stage rotation axis and the side of interest.[19] Equation 2 is derived by considering the fact that the sample stage is tilted clockwise and thus the coordinates of the particle at 60° tilt can be described by transforming the coordinates of the 0° tilt by a counterclockwise rotation.

Comparison of Simulated and Experimental Data. For the comparison of measurement data with simulation results, at least 10 particles for each chemical species, in different size ranges, were measured. The size and shape of the particles were determined by using secondary electron images taken at 0 and 60° sample stage tilts. Also, the characteristics of the detector used in this work was determined by using the measurement data for all the compounds. The detection of the low-energy X-rays is very sensitive to the type and status of the EDX detector. However, it is common that the manufacturer of the detector does not provide detailed information on the detector, so that accurate simulation for the low-energy X-rays is hindered by the uncertain detector efficiency. Furthermore, contaminants, mostly organic carbon from rotary pump oil, and moisture in the chamber form a film on the detector surface. The additional film reduces X-ray intensities, affecting low-energy X-rays mostly.[20] The simulated data were scaled to provide the best match with the measured data iteratively by varying the characteristics of the detector. The obtained detector parameters are as follows: the thickness of gold contact is 7 nm and the silicon dead layer 90 nm, which are less than the values provided by the manufacturer by a factor of ~2. Since the detector was operated in windowless mode, the carbon contamination layer on the detector is also not negligible; a contamination layer thickness of 80 nm was used in our simulations.

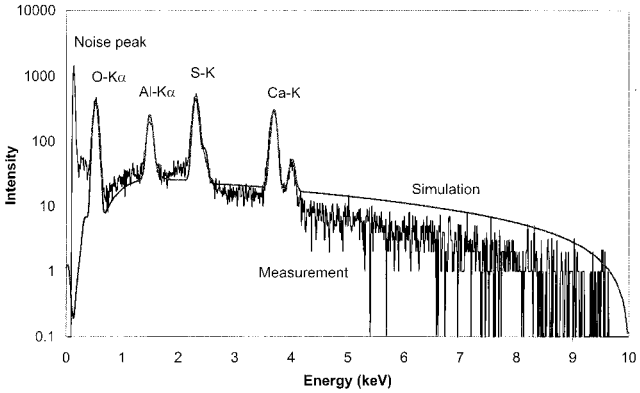

Figure 5. Comparison of simulated and measured spectra for a single $CaSO_4$ particle.

Table 1. Standard Deviation of Particle Size and Standard Deviation of the Ratio between Measured and Simulated X-ray Intensities at 10-keV Excitation Energy (in %)

	particle size			elemental intensities					
composition	*x*	*y*	*z*	C	O	Na	S	Cl	Ca
$CaCO_3$	53.1	51.5	56.9	11.9	19.9				24.6
$CaSO_4 \cdot 2H_2O$	119.9	44.1	92.6		15.8		27.7		19.7
NaCl	68.9	65.1	126.0			12.9		19.5	

In Figure 5, it is shown that there is a quite reasonable match between simulated spectra using the corrected detector efficiency data and measured spectra, including the Bremsstrahlung background. Since the generation mechanism of characteristic X-rays is different from that of Bremsstrahlung,[21] the reasonable agreement in the whole spectra is an indication for the validity of the Monte Carlo calculation.

In Table 1 the standard deviation of size and the standard deviation of the ratios between measured and simulated intensities are shown. Although the sizes of particles vary much, the ratios, which are measures for the goodness of the simulation to the measured data, are relatively constant. In other words, the size effect on X-ray intensities is well simulated in the Monte Carlo

(19) Arfken, G. B. *Mathematical Methods for Physicists*, 2nd ed.; Academic Press: New York, 1970.

(20) Freeman, G. B.; Starr, T. L.; Lackey, W. J.; Hanigofsky, J. A. *Microbeam Anal.* **1994**, *3*, 31−40.

(21) Goel, S. K.; Singh, M. J.; Shanker, R. *Phys. Rev.* **1995**, *A52*, 2453−2456.

Table 2. Ratios between Measured and Simulated X-ray Intensities at 10-kV Acceleration Voltage[a]

composition	C Kα 0.277 keV	O Kα 0.525 keV	Na Kα 1.041 keV	Si Kα 1.740 keV	S Kα 2.307 keV	Cl Kα 2.622 keV	Ca Kα 3.691 keV	Ba Lα 4.464 keV	Fe Kα 6.399 keV
SiO_2		1.10		1.24					
		(0.10)		(0.15)					
Fe_2O_3		0.97							0.94
		(0.19)							(0.15)
$BaSO_4$		1.02			0.93			0.94	
		(0.43)			(0.34)			(0.23)	
$CaSO_4 \cdot 2H_2O$		1.23			1.08		0.97		
		(0.26)			(0.26)		(0.19)		
$CaCO_3$	2.31	1.05					0.77		
	(0.16)	(0.21)					(0.24)		
NaCl			1.01			0.91			
			(0.13)			(0.20)			

[a] Relative standard deviations in parentheses.

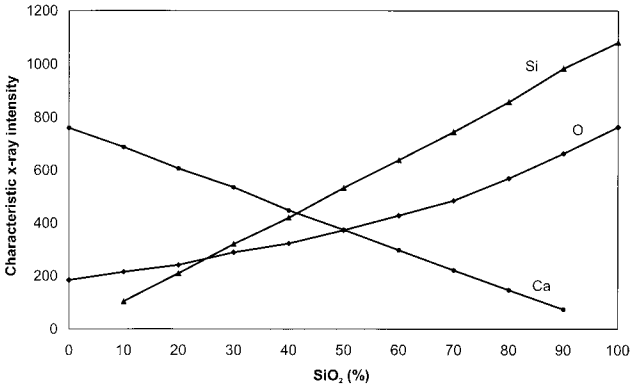

Figure 6. Simulated X-ray intensities of 2-μm-diameter spherical particles with different amounts of two components, CaO and SiO_2.

calculation. Table 2 shows the ratios of the measured and simulated characteristic intensities for each element present in the studied compounds. Except carbon Kα, all the measured X-ray intensities are well simulated by the Monte Carlo calculation. This result indicates that the Monte Carlo method can be applied for the analysis of microparticles if the geometry of particles is accurately determined. For the carbon Kα, the measured intensity is larger than the simulated one by a factor of ~2. The reason is mainly because of the carbon cracking on the particles from organic contamination of the sample and rotary pump oil. And also it may be due to the large uncertainty of the available mass absorption coefficient data for the low-*Z* elements. The uncertainty of the mass absorption coefficient data for the low-*Z* elements in the literature may exceed 30%.[22]

Monte Carlo Calculation for the Speciation of Microparticles. The Monte Carlo simulation is a reliable tool to evaluate the matrix and geometric effects for individual particles. For example, a series of simulations on particles, composed of CaO and SiO_2 in different ratios, was carried out. Figure 6 shows a simulation result, for spherical particles of 2-μm-diameter. X-ray intensities for Ca and Si vary almost linearly as their concentration changes. Oxygen is present in both species, and yet the intensity is different by the factor of 5 when the composition of the particle changes from the particle of one species to that of the another. Also, it is observed that the intensity varies nonlinearly as the concentration changes. In other words, the X-ray intensity of the light element is affected more by the matrix effect even in a microscopic volume. The variation of intensities according to the concentration variation is significant, so that the determination of the concentration of each species is straightforward, if the accurate geometry of a particle is known; the intensity variation due to size and shape variations is more pronounced for submicrometer particles than that of concentration variation (see Figure 3b).

The method based on measurements of particulate standards and Monte Carlo calculation was applied for the speciation of individual aerosol particles collected on a roof of the University of Antwerp, which is located in a suburban region of the city. X-ray spectra were collected with 10-kV accelerating voltage, 1-nA beam current, and 50-s live time for each particle. The net X-ray intensities for the elements were obtained by nonlinear least-squares fitting using the AXIL program.[23] The size and shape parameters of the particles were determined from two secondary electron images for each particle, as described above. The composition of the particles was determined by iterative simulations. However, the aluminum intensities were not included in the calculation, because aluminum foil is used as collecting substrate. The iteration was carried out in the following way: The initial weight fractions of the elements present in the particle were the measured net characteristic intensity values normalized to 1. The first simulation used the weight fractions as input to calculate a new set of intensities. For the next iteration, the weight fractions were modified by multiplying the ratio between the measured intensities and the intensities obtained by the simulation and normalized to 1. The iteration stopped when the differences of the weight fraction values between the iterations were within 1% for each element. As an example, results for two particles are shown in Table 3. Although the examples are nearly spherical particles, the method was successfully applied to irregularly shaped particles as well. Particle A contains ~93% Fe_2O_3 and ~7% SiO_2. Particle B is a fly ash particle, containing mostly aluminosilicate and also small amounts of Na, Mg, Ti, and V. The aluminum intensities were taken into account in the simulation for particle B, because the sum of the intensities was 20% less

(22) Bastin, G. F.; Heijligers, H. J. M. In *Electron Probe Quantitation*; Heinrich K. F. J., Newbury, D. E., Eds.; Plenum Press: New York, 1991; pp 145−161.

(23) Van Espen, P.; Janssens, K.; Nobels, J. *Chemom. Lab.* **1987**, *1*, 109−114.

Table 3. Examples for Aerosol Particle Analysis Using the Monte Carlo Method

element	intensity measd	intensity simul	rel diff between measd and simul intens (%)	wt fraction (%)
Particle A, Diameter 5 μm, Spherical				
O	22137	21976	0.7	24.4
Si	2748	2715	1.2	3.2
Fe	4704	4641	1.3	72.4
Particle B, Diameter 3 μm, Spherical				
O	35115	33936	3.3	45.2
Na	5204	5033	3.3	5.9
Mg	766	739	3.5	0.8
Al	19976	19433	2.7	21.1
Si	21765	21000	3.5	25.3
Ti	134	131	2.2	0.5
V	202	199	1.5	1.1

when aluminum was not included in the calculation. It is demonstrated that the Monte Carlo method combined with particulate standard measurements is capable of semiquantitative determination of light elements in single microscopic particles.

CONCLUSIONS

After accurate determination of the detector efficiency function using the measurement data from standard particles, the geometric and matrix effects for microparticles are well characterized by the Monte Carlo calculation. Systematic modeling for the geometric and matrix effects by using a large number of simulations is expected, with the parametrization of those effects based on chemical compositions, to allow a more convenient and accurate speciation of particles. Also, it is necessary to study how accurately the Monte Carlo calculation can quantify each chemical composition of microparticles in an internal mixture. In atmospheric pollution, many of the most important pollutants are composed of the light elements, such as ammonium sulfate and ammonium nitrate. Since the ammonium compounds are volatile under the vacuum and easily damaged by the electron beam, the analysis of those particles requires the use of a cold stage, to measure them at liquid nitrogen temperature, which is the topic of our next research. The Monte Carlo calculation, developed for the light element analysis here, will be a valuable tool to obtain detailed information on aerosol particles with light elements.

ACKNOWLEDGMENT

This work was partially financed by the Belgian State Office for Scientific, Technical and Cultural Affairs through a research project (in the framework of the program “Sustainable Management of the North Sea”; Contract MN/DD/10) and through a research grant to J.O. and partially by the European Union through Project ENV4-CT95-0088. The support of the Hallym Academy of Sciences, Hallym University, Korea, is also highly appreciated.

Received for review September 28, 1998. Accepted February 2, 1999.

AC981070F